Structure and Energetics of Group 14 (IV-A) Halides: A Comparative Density Functional-Pseudopotential Study

Sigfrido Escalante

Departamento de Química Inorgánica, Posgrado, Facultad de Química, Universidad Nacional Autónoma de México, México D.F. 04510, Mexico

Rubicelia Vargas

Departamento de Química, Universidad Autónoma Metropolitana−Iztapalapa, A.P. 55−534, México D.F. 09340, Mexico

Alberto Vela*

Departamento de Química, Centro de Investigación y de Estudios Avanzados del I.P.N., A.P. 14−740, México D.F. 07000, Mexico

Received: April 7, 1999

The complete set of MX_2 and MX_4 (M = C, Si, Ge, Sn, Pb and X = F, Cl, Br, I) group 14 halides are studied with density functional theory and quasirelativistic effective core potentials. To analyze the role of density inhomogeneities and the asymptotic behavior of the Kohn−Sham effective potential in these molecules, the following exchange-correlation energy functionals are tested: local, semilocal (generalized gradient), and hybrid functionals. For comparison, Hartree−Fock results are also presented. Fully optimized geometries are in very good agreement with experimentally available data and with other high-level theoretical calculations. The energy differences associated with the dissociation and disproportionation reactions are reported. Zero-point corrections and atomic spin−orbit effects are included in these reaction energies. The dissociation energies predicted at the Hartree−Fock level are underestimated, the local energy differences are overestimated, and both the semilocal and hybrid approaches provide the best estimates for these reaction energies. The disproportionation energies, which are commonly used to explore the relative stability of different atomic valences, show a behavior that departs from that commonly known for reactions involving a single atom: the local and semilocal disproportionation energies have very similar values and follow the same trends.

I. Introduction

Group 14 (IV-A) halides have been studied experimentally and theoretically because some of these compounds are used in several crucial steps in the semiconductor industry.[1,2] From the academic point of view, the study of a family of main group compounds belonging to groups 13 (III-A) and 14 (IV-A) has the additional interesting feature that first-row elements usually have a valence higher than those elements corresponding to the fifth and sixth rows. Thus, boron usually is trivalent and carbon tetravalent, while thallium and lead tend to form stable compounds with +1 and +2 oxidation states, respectively. Basic properties of some of these compounds are unknown or, in the best case, are known with a high degree of inaccuracy. Geometrical and thermodynamic data for several of these substances are missing. The experimental difficulties stem from the instabilities of certain halides; CX_2, where X is a halogen, is a highly reactive molecule[3] and, on the other side, PbX_4 compounds are very rarely known.[4] This later fact results in the unavailability of geometrical (bond distances and angles) and thermodynamic information (heats of formation, bond dissociation energies, and disproportionation reaction energies) that is valuable in the modeling of processes where these species are involved. An example of these processes is the surface reaction that takes place in the etching of semiconductors or the chemical deposition of impurities by three-component plasmas.[5,6]

From the theoretical point of view, previous studies on group 14 hydrides and monoxides using the all-electron Dirac−Hartree−Fock method have addressed the issue of periodic trends in some molecular properties.[7−10] A similarly exhaustive and high-quality study on group 14 halides has not been possible until now. Correlation and relativistic effects are important in many of these halides, but the high number of electrons has made this study unfeasible. Recent advances in the methodology, as well as in basic theory, have shown that density functional theory (DFT) is a practical alternative to incorporate correlation effects in systems with a large number of electrons.[11−14] On the other hand, after several years of work, several groups have been able to generate effective core potentials (ECP)[15,16] including scalar relativistic effects for almost all elements in the periodic table. These two ingredients open the theoretical possibility of approaching problems such as the one considered in the present work.

The considerations raised in the previous paragraph constitute the basic motivation for this work, namely, to study, exhaustively, the capabilities of local, semilocal, and hybrid exchange-correlation functionals, in conjunction with effective core potentials, in describing geometrical and energetic properties

10.1021/jp991172p CCC: $18.00
Published on Web 06/24/1999

of group 14 halides with MX_2 and MX_4 stoichiometries. The structure of this work is as follows. In section II, some theoretical considerations and the computational details are presented. To validate the methodological procedure used in this work, the first ionization potentials and electron affinities of groups 14 and 17 elements, as well as the molecular constants for the halogen diatomics are presented at the beginning of section III. The results for optimized geometries, dissociation energies, and disproportionation energies of group 14 elements are presented and compared with available experimental and theoretical data in section III. The roles of relativity and of different approximations to the exchange-correlation energy functional in the calculation of the molecular properties described above are discussed in section IV. Finally, the conclusions of this work are presented in section V.

II. Theoretical and Computational Approach

To analyze the role of correlation, density inhomogeneities, and the asymptotic behavior of the Kohn−Sham effective potential in the calculation of structural and energetic data of group 14 halides, the following exchange-correlation energy functionals are considered in the present work: at the local spin-density approximation level, the parametrization of Vosko, Wilk, and Nusair,[17] which herein will be denoted by LSDA; at the semilocal or generalized gradient approximation (SDA) level, the exchange functional proposed by Becke[18] and Lee, Yang, and Parr's[19] correlation functional (BLYP) and, finally, the three-parameter hybrid functional with the same exchange and correlation as that in SDA (B3LYP).[20] Effective core potentials (ECP) are used to represent the inner electrons of all atoms in the molecules calculated in the present work. ECPs and basis sets are from Stoll and Preuss.[21] The basis sets of all halogen atoms were extended with an extra polarization function.[22] The exponents for F−Br were taken from ref 23 and those for iodine from ref 24. Recently, it has been suggested that the basis sets used in conventional wave function calculations with ECPs similar to those used in this work are not completely appropriate for DFT calculations.[25] However, in the present calculations, no basis optimization was done. It is worth noting that these ECPs have been widely used to study relativistic effects at the Möller−Plesset or configuration interaction levels of theory, but to the authors' knowledge, there are only two works in the literature that have used these ECPs in conjunction with DFT calculations.[26,27] To analyze the role of relativity, nonrelativistic (NR) and quasirelativistic (QR) calculations were done at all theoretical levels. Thus, a byproduct of the present study is to validate the use of these ECPs together with a DFT approach to include relativistic and correlation effects. In the rest of this work, the theoretical model will be denoted by two strings separated by a dash. The first string will denote the exclusion (NR) or inclusion (QR) of scalar relativistic effects through the ECP, and the second string refers to the exchange-correlation functional (LSDA, BLYP, B3LYP) or Hartree−Fock (HF). Kohn−Sham equations are solved within the linear combination of Gaussian-type orbitals approximation using the ECPs and exchange-correlation functionals mentioned above. The numerical integrations were done with a FineGrid that is comprised of 75 radial points and 302 angular points per shell. All the calculations presented in this work were done with Gaussian.[28]

III. Results

III.1. Elements and Diatomic Molecules. In this section, results using nonrelativistic (NR) and quasirelativistic (QR) effective core potentials are presented for the set of molecules MX_2 and MX_4. As mentioned in the Introduction, few reliable experimental data for these systems are known. Thus, a statistically valid comparison is not possible either for the structural or energetic quantities calculated in this work. To gain some confidence on the theoretical models used, the ionization potentials (see Table 1) and electron affinities (see Table 2) of the group 14 and group 17 atoms were calculated with the theoretical models proposed in the previous section. For both sets of elements, the calculated ionization potentials are in good agreement with experiment. The largest average absolute deviations are 0.53 eV, corresponding to the NR-LSDA values of group 14 elements, and 1.55 eV, corresponding to the NR-HF calculations of the halogen atoms. Turning to the electron affinities, the theoretical models considered in this work tend to underestimate the electron affinities of these atoms. The largest average absolute deviations in this case are 0.84 eV (QR-HF), corresponding to the group 14 elements, and 2.0 eV (NR-HF) for the halogens. It is worth noting that, for practically all theoretical models, the calculated electron affinities of C and F show the largest deviations from the experimental value. In Table 3, the bond distances, dissociation energies, and frequencies of the halogen diatomic molecules are presented. The average absolute deviations of these quantities are presented in Table 4. Calculated bond distances are in general good agreement with experiment. In all cases, and as expected, the QR bond distances are closer to experiment than the nonrelativistic ones. Quasirelativistic HF and LSDA bond distances are very

TABLE 1: Nonrelativistic (NR) and Quasirelativistic (QR) Ionization Potentials of Group 14 and Group 17 Elements Calculated at Hartree−Fock (HF), Local (LSDA), Semilocal (BLYP), and Hybrid (B3LYP) Levels[a]

	HF		LSDA		BLYP		B3LYP		
atom	NR	QR	NR	QR	NR	QR	NR	QR	exptl
Group 14 (IV-A)									
C	10.98	10.88	12.05	11.95	11.36	11.26	11.56	11.45	11.26
Si	7.85	7.76	8.74	8.62	8.11	8.02	8.29	8.20	8.15
Ge	7.55	7.50	8.42	8.38	7.86	7.81	8.02	7.97	7.90
Sn	7.02	6.97	7.88	7.84	7.30	7.26	7.46	7.43	7.34
Pb	6.79	6.64	7.64	7.56	7.05	6.99	7.22	7.13	7.42
Group 17 (VII-A)									
F	15.69	15.70	18.01	17.99	17.11	17.08	17.30	17.28	17.42
Cl	12.06	11.86	13.77	13.59	13.04	12.84	13.24	13.04	12.97
Br	10.16	10.94	11.92	12.62	11.15	11.88	11.33	12.07	11.81
I	8.54	9.64	10.22	11.25	9.51	10.55	9.66	10.73	10.45

[a] The experimental values are from ref 33. All quantities are in eV.

TABLE 2: Nonrelativistic (NR) and Quasirelativistic (QR) Electron Affinities of Group 14 and Group 17 Elements Calculated at Hartree−Fock (HF), Local (LSDA), Semilocal (BLYP), and Hybrid (B3LYP) Levels[a]

	HF		LSDA		BLYP		B3LYP		
atom	NR	QR	NR	QR	NR	QR	NR	QR	exptl
Group 14 (IV-A)									
C	−0.21	−0.25	0.97	0.94	−0.07	−0.09	0.18	0.15	1.26
Si	0.65	0.60	1.71	1.67	0.85	0.80	1.04	0.98	1.24
Ge	0.71	0.48	1.86	1.56	1.02	0.72	1.17	0.89	1.20
Sn	0.55	0.53	1.56	1.54	0.74	0.73	0.93	0.91	1.25
Pb	0.59	0.44	1.54	1.46	0.75	0.68	0.94	0.85	1.04
Group 17 (VII-A)									
F	−0.30	−0.37	1.97	1.87	0.70	0.59	0.97	0.87	3.40
Cl	2.14	2.03	3.95	3.85	2.97	2.86	3.19	3.07	3.62
Br	1.83	2.19	3.66	3.91	2.70	2.99	2.89	3.20	3.36
I	1.80	2.15	3.58	3.81	2.69	2.93	2.84	3.12	3.06

[a] The experimental values are from ref 33. All quantities are in eV.

TABLE 3: Nonrelativistic (NR) and Quasirelativistic (QR) Bond Distances, Dissociation Energies Including Zero-Point Energy Corrections (D_0), and Harmonic Frequencies of Halogen Diatomic Molecules Calculated at Hartree−Fock (HF), Local (LSDA), Semilocal (BLYP), and Hybrid (B3LYP) Levels[a]

	HF		LSDA		BLYP		B3LYP		
molecule	NR	QR	NR	QR	NR	QR	NR	QR	exptl
				Bond Distances/Å					
F_2	1.334	1.3355	1.3854	1.3865	1.4281	1.4298	1.3964	1.3979	1.41193
Cl_2	1.9788	1.9955	2.0158	2.0327	2.0643	2.0816	2.0313	2.0488	1.987
Br_2	2.3507	2.283	2.3754	2.3043	2.4285	2.3528	2.3959	2.3237	2.281
I_2	2.7987	2.7062	2.8231	2.7174	2.8813	2.77	2.8458	2.7409	2.666
				Dissociation Energies (D_0)/kJ mol^{-1}					
F_2	−155.26	−154.63	331.53	331.05	190.93	189.52	141.30	140.37	154.77
Cl_2	47.80	40.38	322.64	318.42	214.08	208.05	200.28	193.81	239.66
Br_2	60.72	47.60	291.37	293.51	192.52	196.16	184.25	184.66	190.16
I_2	70.40	45.21	260.74	257.11	171.03	168.11	167.75	160.05	148.95
				Frequencies/cm^{-1}					
F_2	1224.37	1223.27	1060.82	1058.32	964.35	960.85	1039.14	1036.35	919.00
Cl_2	620.96	609.29	550.82	541.16	495.61	486.86	534.80	524.62	559.71
Br_2	335.78	356.36	306.26	329.96	272.12	297.10	293.82	317.48	323.33
I_2	224.61	233.94	205.07	220.40	183.51	198.56	197.55	210.90	214.52

[a] The experimental values are from ref 38.

TABLE 4: Average Absolute Deviations of the Bond Distances, Dissociation Energies, and Frequencies for the Halogen Diatomic Molecules

	HF		LSDA		BLYP		B3LYP	
	NR	QR	NR	QR	NR	QR	NR	QR
bond distances (Å)	0.0721	0.0318	0.0767	0.0365	0.1141	0.0721	0.0886	0.0484
dissociation energies (kJ mol^{-1})	177.5	188.7	118.2	116.7	21.6	22.9	19.4	19.2
frequencies (cm^{-1})	97.29	101.57	44.31	42.59	47.92	39.22	47.88	40.48

similar to each other and have the smallest absolute errors. The hybrid method (B3LYP) predicts better distances than its related SDA (BLYP), but they are not better than those provided at the HF and LSDA levels. HF dissociation energies are severely underestimated. Special attention deserves F_2, where both NR-HF and QR-HF results predict, in agreement with Dolg,[29] a negative binding energy for this diatomic molecule. In agreement with many works, LSDA dissociation energies are too large and the gradient corrections improve considerably the values for this quantity. B3LYP dissociation energies are the best, with a 19.2 kJ mol^{-1} absolute error in the quasirelativistic method. For all the theoretical methods considered here, the calculated harmonic frequencies decrease as one moves down the periodic table. HF frequencies are always overestimated. All calculated frequencies for F_2 are greater than the experimental values. With the exception of F_2, BLYP and B3LYP harmonic frequencies are underestimated. As can be seen in Table 4, in general, DFT frequencies are closer to the experimental values. The average absolute deviation from experiment is reduced by more than half when compared with HF. The smallest deviation obtained in the calculation of this quantity corresponds to the semilocal functional (QR-BLYP), followed very closely by the quasirelativistic hybrid method (QR-B3LYP). Overall, the atomic and halogen diatomic calculations show that the energetical description of group 14 isolated atoms and halogen diatomics is well described by the quasirelativistic hybrid method. The structural parameters (bond distances) of group 17 diatomics are equally well described by QR-HF and QR-LSDA, with the hybrid functional being very close behind.

III.2. Geometries. Full geometry optimizations with analytic gradients were performed on the dihalides and tetrahalides. The point group used for the latter molecules is T_d, and the multiplicity of all the molecules reported in this work is one, i.e., all molecules are in the singlet state. To characterize the nature of each extreme and to evaluate the zero-point energy (ZPE), the harmonic analysis was done on every molecule and for each theoretical level. In all cases, the T_d structures are minima in the potential energy surface. The optimized NR and QR bond distances and bond angles for the MX_2 molecules are presented in Tables 5 and 6, respectively, and those corresponding to the bond distances of MX_4 are shown in Table 7. The average absolute deviations of the quasirelativistic optimized geometrical parameters, with respect to other theoretical calculations and experimental data,[30] are reported in Table 8. On doing this comparison with other theoretical works, the primary intention was to compare with ab initio calculations available in the literature. As can be seen in Tables 5−7, the number of multireference calculations for the dihalides allows one an almost complete comparison with this theoretical method. For the tetrahalides, there is only one multireference calculation reported in the QCLDB.[31] Consequently, a comparison similar to that performed for the dihalides is not possible, and thus, SCF values were used to obtain the average absolute deviations of MX_4 bond distances. From the deviations reported in Table 8, one can see that in general, HF bond distances, calculated with the present methodology, are the best, reflecting that the electronic structure of the tetrahalides is very well described at this level. With the density functional methods, the local and hybrid exchange-correlation functionals provide very similar bond distances, which in the worst case are 0.017 Å away from the HF value. Interestingly, the semilocal functional used in this work has the largest deviations, and thus, it should not be recommended to optimize geometries of similar compounds when using the present methodology. To illustrate the behavior of the bond distances for MX_2, the results corresponding to HF are depicted in Figure 1, and for MX_4 (T_d) molecules, those at the LSDA level are depicted in Figure 2. All theoretical levels show very similar trends, reproducing the experimental one. As can be seen in Figure 1, there is one molecule, namely CBr_2, that clearly departs from the calculated trends. In view of the good description obtained for the other molecules and the agreement of the present calculations with other high-quality

TABLE 5: Nonrelativistic (NR), Quasirelativistic (QR), Experimental, and Other Theoretical Bond Distances (in Å) of MX_2 Molecules Calculated at Hartree−Fock (HF), Local (LSDA), Semilocal (BLYP), and Hybrid (B3LYP) Levels

	HF		LSDA		BLYP		B3LYP			
molecule	NR	QR	NR	QR	NR	QR	NR	QR	exptl[a]	other works[b]
CF_2	1.2649	1.2729	1.3009	1.3082	1.3169	1.3246	1.2971	1.3048	1.3035 (mw) [39]	1.347 (MR)[40] 1.299 (CAS)[41]
CCl_2	1.6927	1.7106	1.7385	1.7523	1.769	1.7836	1.737	1.7525	1.7157 (mw) [42]	1.756 (MR)[40] 1.713 (CISD)[42]
CBr_2	1.8776	1.8756	1.9257	1.9143	1.9602	1.9485	1.9242	1.9167	1.74 (eldiff) [43]	1.958 (MC)[43]
CI_2	2.0791	2.1116	2.132	2.1454	2.1679	2.1828	2.1254	2.1496		
SiF_2	1.5968	1.5909	1.6283	1.6242	1.6343	1.6305	1.6195	1.6149	1.591 (mw) [44]	1.584 (CISD)[44] 1.5798 (CAS)[45]
$SiCl_2$	2.067	2.0829	2.097	2.1155	2.118	2.1368	2.0961	2.1138	2.0653 (mw) [46]	2.073 (MP2)[46]
$SiBr_2$	2.2728	2.2563	2.3031	2.2821	2.3314	2.3087	2.3068	2.2847	2.24 [47]	2.257 (MP2)[48]
SiI_2	2.5186	2.5067	2.5438	2.5229	2.581	2.5589	2.552	2.5324		2.5 (HF)[47]
GeF_2	1.7474	1.7549	1.7845	1.7849	1.7942	1.7934	1.7759	1.7771	1.732 (mw)[49]	1.723 (MR)[50] 1.732 (CCSD)[49]
$GeCl_2$	2.1964	2.209	2.2217	2.2329	2.2473	2.2586	2.2249	2.2359	2.1694 (mw)[51]	2.191 (MR)[34]
$GeBr_2$	2.3921	2.369	2.4146	2.3842	2.4487	2.4149	2.4234	2.3919	2.337 [52]	2.373 (MR)[34]
GeI_2	2.6309	2.6062	2.6459	2.6108	2.6883	2.6479	2.6602	2.6242	2.54[53]	2.574 (MR)[34]
SnF_2	1.8874	1.9238	1.9163	1.9585	1.92	1.9641	1.9065	1.9477		1.865 (MR)[50]
$SnCl_2$	2.3313	2.3926	2.3544	2.4171	2.371	2.4378	2.3527	2.4166	2.347 (eldiff)[54]	2.363 (MR)[c] 2.073 (MP2)[46]
$SnBr_2$	2.5315	2.547	2.5531	2.5628	2.5783	2.588	2.5569	2.567	2.504[c]	2.535 (MR)[c]
SnI_2	2.7693	2.7786	2.7864	2.785	2.821	2.8182	2.7956	2.7955	2.699[c]	2.738 (MR)[c]
PbF_2	1.9725	1.9998	2.0168	2.0279	2.0196	2.0352	2.0014	2.0183	2.033 (eldiff)[55]	2.139 (MR)[50] 2.047 (MP2)[35]
$PbCl_2$	2.4628	2.4912	2.4932	2.4988	2.5087	2.5234	2.4888	2.505	2.46[c]	2.542 (MR)[c]
$PbBr_2$	2.6626	2.6402	2.6931	2.6383	2.7183	2.667	2.6942	2.6485	2.6[c]	2.684 (MR)[c]
PbI_2	2.8989	2.8611	2.9255	2.8493	2.9604	2.8847	2.9324	2.8656	2.79[c]	2.878 (MR)[c]

[a] Experimental values from microwave spectroscopy (mw) or electron diffraction (eldiff). [b] Other theoretical values from multireference (MR), complete active space (CAS), configuration interaction (CISD), Möller−Plesset (MP), or Hartree−Fock (HF) calculations. [c] See ref 56.

TABLE 6: Nonrelativistic (NR), Quasirelativistic (QR), Experimental, and Other Theoretical Bond Angles (in Degrees) of MX_2 Molecules Calculated at Hartree−Fock (HF), Local (LSDA), Semilocal (BLYP), and Hybrid (B3LYP) Levels

	HF		LSDA		BLYP		B3LYP			
molecule	NR	QR	NR	QR	NR	QR	NR	QR	exptl[a]	other works[b]
CF_2	105.0	104.7	104.0	103.8	104.2	103.9	104.4	104.1	104.78 (mw)[39]	103.6 (MR)[40] 104.7 (CAS)[41]
CCl_2	110.3	109.9	108.8	108.6	109.2	109.0	109.4	109.1	109.2[57]	109.4 (MR)[40] 109.4 (CISD)[42]
CBr_2	114.4	110.8	112.2	109.5	112.7	110.3	112.9	110.2	114[43]	110.6 (MR)[43]
CI_2	120.0	112.6	116.4	110.9	116.9	112.2	117.5	111.9		
SiF_2	99.0	98.8	99.9	99.7	100.8	100.7	100.3	100.2	100.8[44]	99.9 (CISD)[44] 99 (CAS)[45]
$SiCl_2$	101.2	101.1	101.0	101.2	102.4	102.7	101.8	102.0	101.5[46]	101.7 (MP2)[46]
$SiBr_2$	103.3	102.0	102.6	102.0	104.4	103.8	103.8	103.0	103[47]	102.2 (MP2)[48]
SiI_2	105.8	103.4	105.4	103.4	107.2	105.7	106.4	104.6		103 (HF)[47]
GeF_2	96.3	96.4	97.5	97.6	98.3	98.4	97.8	97.8	97.2[49]	97.1 (MR)[50] 97.6 (CCSD)[49]
$GeCl_2$	99.7	99.8	99.7	100.0	101.5	101.7	100.6	100.9	99.9[51]	100.5 (MR)[34]
$GeBr_2$	101.8	101.1	101.3	101.1	103.4	103.2	102.6	102.3	101.2[52]	101.8 (MR)[34]
GeI_2	104.4	102.7	104.3	103.1	106.5	105.5	105.5	104.4	102.1[53]	102.8 (MR)[34]
SnF_2	95.3	94.6	96.9	95.8	97.5	96.4	97.0	96.0		92 (MR)[50]
$SnCl_2$	98.2	97.7	98.5	97.9	100.1	99.7	99.3	98.9	99[54]	98.4 (MR)[c] 101.7 (MP2)[46]
$SnBr_2$	100.2	98.8	99.6	98.7	101.9	100.9	101.0	100.0	98.6[c]	99.7 (MR)[c]
SnI_2	102.4	100.5	102.1	100.7	104.5	103.3	103.5	102.3	103.5[c]	100.9 (MR)[c]
PbF_2	93.5	95.4	94.3	95.4	94.7	95.8	94.5	95.8	97.8[55]	98.5 (MR)[50] 96.7 (MP2)[35]
$PbCl_2$	96.1	99.1	96.1	98.6	97.7	100.4	97.0	99.8	96[c]	100.8 (MR)[c]
$PbBr_2$	97.9	100.1	96.8	99.2	99.1	101.5	98.4	100.8	98.8[c]	101.5 (MR)[c]
PbI_2	100.0	101.6	99.2	101.1	101.8	103.9	100.8	103.0	99.7[c]	103.6 (MR)[c]

[a] Experimental values from microwave spectroscopy (mw). [b] Other theoretical values from multireference (MR), complete active space (CAS), configuration interaction (CISD), Möller−Plesset (MP), or Hartree−Fock (HF) calculations. [c] See ref 56.

theoretical predictions, one can conclude that the experimental bond distance of CBr_2 has to be revised. The reported experimental bond distance of carbon dibromide is too small.

Turning to bond angles in MX_2, the nonrelativistic and quasirelativistic values provided by B3LYP are depicted in Figure 3. All theoretical levels have the same general charac-

TABLE 7: Nonrelativistic (NR), Quasirelativistic (QR), Experimental, and Other Theoretical Bond Distances (in Å) of MX_4 Molecules with T_d Symmetry, Calculated at Hartree−Fock (HF), Local (LSDA), Semilocal (BLYP), and Hybrid (B3LYP) Levels

	HF		LSDA		BLYP		B3LYP			
molecule	NR	QR	NR	QR	NR	QR	NR	QR	exptl[a]	other works[b]
CF_4	1.2887	1.2928	1.3164	1.3195	1.3341	1.338	1.3176	1.3214	1.319[58]	1.301 (HF)[58]
CCl_4	1.7517	1.7661	1.7697	1.7819	1.8031	1.8167	1.7808	1.7942	1.769[59]	1.765 (HF)[60]
CBr_4	1.9716	1.9358	1.982	1.9449	2.0241	1.9851	1.9992	1.9616	1.942[60]	1.934 (HF) [60]
CI_4	2.228	2.1866	2.2308	2.1872	2.2813	2.2361	2.2528	2.21	2.1[61]	2.162 (MR)[61]
SiF_4	1.5565	1.5485	1.5838	1.5762	1.5903	1.5826	1.5776	1.5699	1.552[58]	1.557 (HF)[5]
$SiCl_4$	2.0124	2.0246	2.0318	2.0457	2.0505	2.0646	2.0332	2.0466	2.019[59]	2.025 (MP2)[62]
$SiBr_4$	2.2344	2.1999	2.2471	2.2146	2.2763	2.2403	2.2559	2.2204	2.183[c]	2.19 (HF)[c]
SiI_4	2.5032	2.4612	2.5058	2.4661	2.5473	2.5044	2.523	2.4809		
GeF_4	1.6856	1.6887	1.7291	1.7272	1.7379	1.7358	1.7191	1.7183	1.71[63]	1.727 (MP2)[63]
$GeCl_4$	2.1166	2.1291	2.1475	2.1607	2.1715	2.1862	2.1485	2.1623	2.113[c]	2.32 (HF)[64]
$GeBr_4$	2.3331	2.2961	2.3536	2.3196	2.3903	2.3522	2.3643	2.3269	2.272[c]	2.27 (HF)[c]
GeI_4	2.597	2.5473	2.6072	2.56	2.6576	2.6052	2.6275	2.5768	2.507	
SnF_4	1.8329	1.8589	1.8697	1.905	1.8734	1.9103	1.8587	1.892	1.88[58]	1.87 (HF)[58]
$SnCl_4$	2.2504	2.3012	2.2806	2.3396	2.2959	2.3598	2.2769	2.3358	2.28[59]	2.317 (HF)[59]
$SnBr_4$	2.4613	2.4581	2.4857	2.4884	2.5127	2.5142	2.4901	2.4898	2.44 (eldiff)[65]	
SnI_4	2.7174	2.6994	2.7309	2.7179	2.7711	2.7565	2.7446	2.7286	2.64 (eldiff)[65]	
PbF_4	1.9203	1.9162	1.97	1.9805	1.9724	1.9883	1.9538	1.9624		1.972 (MP2)[35]
$PbCl_4$	2.3797	2.3837	2.4184	2.4383	2.4317	2.4676	2.4102	2.4342	2.43[59]	2.345 (MP2)[66]
$PbBr_4$	2.5904	2.5407	2.6237	2.5839	2.6489	2.6197	2.6242	2.5868		
PbI_4	2.8433	2.7789	2.8657	2.8079	2.9041	2.8571	2.8756	2.8218		

[a] Experimental values from electron diffraction (eldiff). [b] Other theoretical values from multireference (MR), complete active space (CAS), configuration interaction (CISD), Möller−Plesset (MP), or Hartree−Fock (HF) calculations. [c] See ref 67.

TABLE 8: Average Absolute Deviations, with Respect to Experiment and Other Theoretical Calculations, of the Bond Distances and Bond Angles of MX_2 and MX_4 Group 14 Halides

	HF		LSDA		BLYP		B3LYP	
	other theoretical calculations	expt	other theoretical calculations	expt	other theoretical calculations	expt	other theoretical calculations	expt
bond distances in MX_2/Å	0.037	0.042	0.043	0.055	0.052	0.079	0.043	0.059
bond angles in MX_2/deg	1.0	1.3	1.1	1.2	1.4	1.9	1.0	1.5
bond distances in MX_4/Å	0.033	0.026	0.037	0.038	0.057	0.065	0.041	0.042

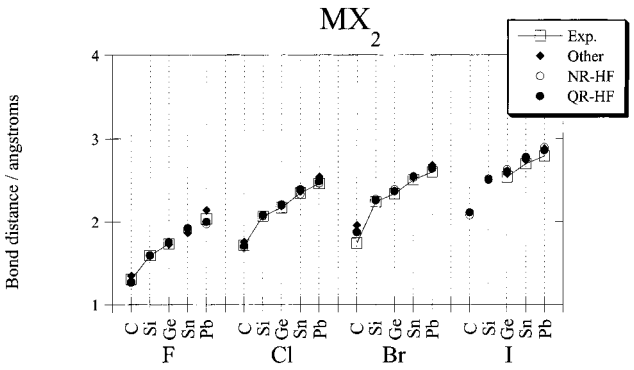

Figure 1. Bond distances for group 14 dihalides calculated with nonrelativistic (NR) and quasirelativistic (QR) effective core potentials and at the Hartree−Fock level; see Table 5.

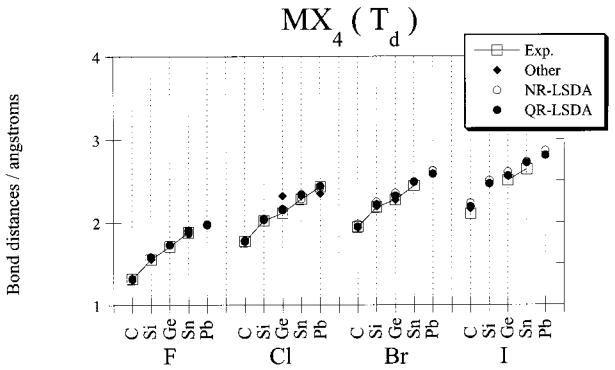

Figure 2. Bond distances for group 14 tetrahalides with tetrahedral symmetry (T_d) calculated with nonrelativistic (NR) and quasirelativistic (QR) effective core potentials and using the local spin-density approximation (LSDA) to the exchange-correlation energy functional; see Table 7.

teristics, being equally satisfactory. The deviation with respect to high-level theoretical calculations is 1.2°, while with respect to experiment it is 1.6°. Again, the largest deviations are obtained with the semilocal functional. For Si and Ge, the theoretical values, particularly the QR ones, are very close to experiment. For a given element belonging to group 14, the bond angle of the dihalide increases upon going from fluorine to iodine. On the other hand, by fixing the halogen atom, it is seen that, in general, the bond angle decreases. For fluorides, there is a monotonic decrease, while for the rest of the halides, the bond angle obtained with the QR pseudopotential of SnX_2 (X = Cl, Br, and I) is minimum. Another interesting feature is that the relativistic corrections in the bond angles of CBr_2 and CI_2 are very substantial. For these molecules, relativity reduces considerably the bond angle. The excellent agreement of the DFT bond length and angle of CBr_2 with high-level ab initio calculations clearly establishes that the experimentally determined structural parameters of this molecule are erroneous. This bond angle contraction is reversed in the case of lead halides. As it can been seen in Figure 3, the QR bond angle of PbX_2 is larger than that predicted without relativistic effects. This behavior is independent of the theoretical model. Thus, concerning the bond angles, one can conclude that relativistic effects are very important for CBr_2, CI_2, and all lead halides. Notice that relativistic trends are different from nonrelativistic in

TABLE 9: Nonrelativistic (NR) and Quasirelativistic (QR) Total Energies (in Atomic Units) of MX_2 Molecules Calculated at Hartree−Fock (HF), Local (LSDA), Semilocal (BLYP), and Hybrid (B3LYP) Theoretical Levels

	HF		LSDA		BLYP		B3LYP	
molecule	NR	QR	NR	QR	NR	QR	NR	QR
CF_2	−53.536	−53.379	−54.412	−54.263	−54.262	−54.109	−54.338	−54.184
CCl_2	−35.127	−34.940	−35.959	−35.771	−35.687	−35.489	−35.779	−35.584
CBr_2	−30.440	−31.669	−31.312	−32.530	−31.015	−32.241	−31.095	−32.323
CI_2	−26.262	−27.710	−27.148	−28.598	−26.831	−28.288	−26.905	−28.362
SiF_2	−51.945	−51.796	−52.785	−52.638	−52.640	−52.490	−52.717	−52.568
$SiCl_2$	−33.565	−33.374	−34.349	−34.158	−34.072	−33.872	−34.171	−33.973
$SiCl_2$	−28.873	−30.106	−29.696	−30.918	−29.389	−30.622	−29.478	−30.713
SiI_2	−24.687	−26.147	−25.524	−26.984	−25.196	−26.664	−25.279	−26.748
GeF_2	−51.836	−51.692	−52.691	−52.554	−52.551	−52.410	−52.621	−52.480
$GeCl_2$	−33.501	−33.321	−34.293	−34.113	−34.018	−33.830	−34.113	−33.927
$GeBr_2$	−28.820	−30.063	−29.649	−30.880	−29.344	−30.587	−29.430	−30.675
GeI_2	−24.644	−26.113	−25.484	−26.953	−25.158	−26.635	−25.239	−26.716
SnF_2	−51.443	−51.268	−52.289	−52.123	−52.152	−51.985	−52.222	−52.053
$SnCl_2$	−33.113	−32.912	−33.896	−33.698	−33.625	−33.419	−33.720	−33.515
$SnBr_2$	−28.429	−29.658	−29.250	−30.469	−28.947	−30.179	−29.033	−30.265
SnI_2	−24.250	−25.712	−25.083	−26.545	−24.757	−26.230	−24.838	−26.310
PbF_2	−51.168	−51.300	−52.006	−52.161	−51.871	−52.021	−51.941	−52.088
$PbCl_2$	−32.844	−32.963	−33.624	−33.752	−33.354	−33.472	−33.448	−33.567
$PbBr_2$	−28.165	−29.714	−28.982	−30.526	−28.680	−30.235	−28.765	−30.321
PbI_2	−23.991	−25.773	−24.818	−26.606	−24.493	−26.290	−24.574	−26.370

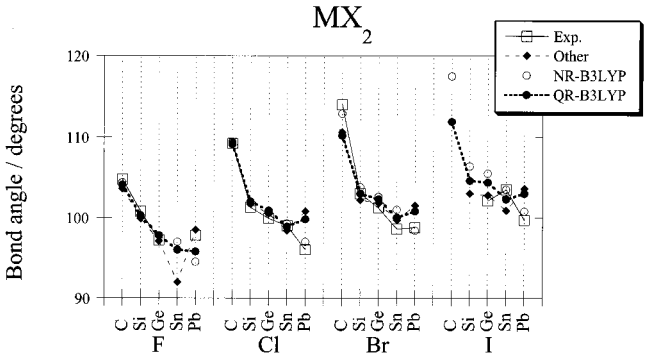

Figure 3. Bond angles for group 14 dihalides calculated with nonrelativistic (NR) and quasirelativistic (QR) effective core potentials and using the hybrid (B3LYP) exchange-correlation energy functional; see Table 6.

halocarbenes, but even for the rest of group 14 elements, there are slight differences between the NR and QR trends.

The discussion in the last two paragraphs allows one to conclude that HF and LSDA are excellent theoretical levels for geometry optimizations of this type of compound within the pseudopotential approach. The hybrid exchange-correlation energy functional is very close behind in the description of structural parameters of group 14 halides.

III.3. Energy Differences for Several Reactions of Group 14 Halides. The nonrelativistic and quasirelativistic total energies and their associated zero-point energies for MX_2 and MX_4 molecules are presented in Tables 9−12. In this section, the energy differences associated with several reactions are presented and discussed. As it was mentioned in the Introduction, these reactions are important in several technological processes and to analyze the valence stability of group 14 elements. For the sake of brevity, the discussion will focus on the energy differences that include the zero-point energies (ZPE) and the atomic spin−orbit (SO) relativistic corrections. The atomic SO values were taken from ref 32.

The dissociation reaction

$$MX_m(g) \rightarrow M(g) + mX(g), \quad D_0 \qquad (1)$$

will be analyzed first. For the di- and tetrahalides, the trends obtained in the calculation of the dissociation energies with the theoretical levels considered in this work are essentially the same. To illustrate this behavior, the dissociation energies of MX_4 are depicted in Figure 4. A general feature that emerges from this figure is that HF underestimates the dissociation energies, the local functional overestimates this quantity, and the values provided at semilocal and hybrid levels are approximately the same. The LSDA overestimation of this energy difference is a well-documented fact. However, it is a little surprising that the dissociation energies provided by the hybrid functional are not substantially different from those obtained at the semilocal level. It could be interesting to test other semilocal and hybrid functionals to determine if this similarity holds. It is also worth noting that, for all tetrahalides, the dissociation energies of the corresponding SiX_4 are a maximum.

From the dissociation energies (D_0), the corresponding mean bond dissociation energies are calculated as

$$\mathrm{BDE} = D_0/m \qquad (2)$$

Mean bond dissociation energies (BDE) are very important in the modeling of several reactions. A source of information for these energies is the data collected by Huheey.[33] As can be seen in Table E.1 of ref 33, the reliability of the BDE for the compounds studied in this work is not uniform. Thus, a full set of BDEs provided by a common high-quality theoretical calculation can help to assess the accuracy of the data reported in the literature. The calculated mean bond dissociation energies for MX_2 and MX_4 group 14 halides are presented in Table 13. The comparison with the experimentally available information shows the same tendencies as that observed in D_0, i.e., HF underestimates, LSDA overestimates, and BLYP and B3LYP are very close to each other and to experiment. All the functionals tested reproduce the experimental tendencies; contrary to HF that for Sn and Pb predicts a totally different trend. The average absolute deviations of the QR-ZPE-SO mean bond dissociation energies, with respect to experiment, in kJ mol^{-1}, are as follows: 151.0 (HF), 85.3 (LSDA), 19.7 (BLYP), and 23.4 (B3LYP), for the MX_2 compounds; for the tetrahalides, one obtains 158.2 (HF), 57.7 (LSDA), 33.1 (BLYP), and 37.2 (B3LYP). Balasubramanian[34] has calculated the bond dissocia-

TABLE 10: Nonrelativistic (NR) and Quasirelativistic (QR) Total Energies (in Atomic Units) of MX_4 Molecules Calculated at Hartree−Fock (HF), Local (LSDA), Semilocal (BLYP), and Hybrid (B3LYP) Theoretical Levels

	HF		LSDA		BLYP		B3LYP	
molecule	NR	QR	NR	QR	NR	QR	NR	QR
CF_4	−101.735	−101.442	−103.303	−103.023	−103.039	−102.751	−103.182	−102.894
CCl_4	−64.9090	−64.5507	−66.3860	−66.0235	−65.8745	−65.4935	−66.0523	−65.6770
CBr_4	−55.5418	−58.0144	−57.0898	−59.5410	−56.5261	−58.9959	−56.6847	−59.1578
CI_4	−47.2003	−50.1080	−48.7612	−51.6767	−48.1600	−51.0903	−48.3084	−51.2374
SiF_4	−100.207	−99.9303	−101.704	−101.431	−101.472	−101.194	−101.616	−101.339
$SiCl_4$	−63.4281	−63.0578	−64.8179	−64.4468	−64.3157	−63.9283	−64.5041	−64.1209
$SiCl_4$	−54.0463	−56.5132	−55.5112	−57.9595	−54.9474	−57.4202	−55.1180	−57.5919
SiI_4	−45.6774	−48.5910	−47.1674	−50.0860	−46.5601	−49.4985	−46.7193	−49.6559
GeF_4	−99.9580	−99.6827	−101.484	−101.220	−101.262	−100.991	−101.392	−101.121
$GeCl_4$	−63.2910	−62.9375	−64.6932	−64.3379	−64.1978	−63.8252	−64.3788	−64.0110
$GeBr_4$	−53.9429	−56.4184	−55.4145	−57.8724	−54.8572	−57.3389	−55.0222	−57.5051
GeI_4	−45.6074	−48.5214	−47.0972	−50.0209	−46.4954	−49.4391	−46.6509	−49.5920
SnF_4	−99.5820	−99.2345	−101.093	−100.760	−100.881	−100.544	−101.010	−100.670
$SnCl_4$	−62.9221	−62.5213	−64.3091	−63.9104	−63.8231	−63.4087	−64.0032	−63.5913
$SnBr_4$	−53.5690	−56.0154	−55.0254	−57.4549	−54.4751	−56.9306	−54.6397	−57.0950
SnI_4	−45.2224	−48.1296	−46.7012	−49.6132	−46.1036	−49.0378	−46.2588	−49.1902
PbF_4	−99.2964	−99.1614	−100.786	−100.714	−100.581	−100.500	−100.712	−100.618
$PbCl_4$	−62.6436	−62.4907	−64.0195	−63.9010	−63.5412	−63.4042	−63.7200	−63.5792
$PbBr_4$	−53.3000	−56.0005	−54.7446	−57.4576	−54.2010	−56.9381	−54.3646	−57.0960
PbI_4	−44.9633	−48.1344	−46.4294	−49.6315	−45.8368	−49.0607	−45.9916	−49.2078

TABLE 11: Zero-Point Energies (in Atomic Units) of MX_2 Molecules Calculated at Hartree−Fock (HF), Local (LSDA), Semilocal (BLYP), and Hybrid (B3LYP) Theoretical Levels

	HF		LSDA		BLYP		B3LYP	
molecule	NR	QR	NR	QR	NR	QR	NR	QR
CF_2	0.0080	0.0078	0.0070	0.0069	0.0066	0.0065	0.0071	0.0070
CCl_2	0.0046	0.0045	0.0040	0.0040	0.0037	0.0037	0.0040	0.0040
CBr_2	0.0036	0.0036	0.0032	0.0033	0.0029	0.0030	0.0031	0.0032
CI_2	0.0029	0.0029	0.0026	0.0027	0.0023	0.0024	0.0025	0.0026
SiF_2	0.0050	0.0051	0.0046	0.0046	0.0045	0.0045	0.0047	0.0047
$SiCl_2$	0.0030	0.0029	0.0027	0.0027	0.0026	0.0025	0.0027	0.0027
$SiCl_2$	0.0023	0.0022	0.0021	0.0021	0.0019	0.0019	0.0021	0.0020
SiI_2	0.0019	0.0018	0.0017	0.0017	0.0016	0.0016	0.0017	0.0017
GeF_2	0.0038	0.0038	0.0034	0.0035	0.0033	0.0034	0.0035	0.0036
$GeCl_2$	0.0022	0.0022	0.0021	0.0021	0.0019	0.0019	0.0020	0.0020
$GeBr_2$	0.0016	0.0016	0.0015	0.0015	0.0014	0.0014	0.0014	0.0015
GeI_2	0.0013	0.0012	0.0012	0.0012	0.0011	0.0011	0.0012	0.0012
SnF_2	0.0036	0.0034	0.0033	0.0031	0.0033	0.0030	0.0034	0.0032
$SnCl_2$	0.0020	0.0019	0.0019	0.0018	0.0018	0.0017	0.0019	0.0018
$SnBr_2$	0.0014	0.0013	0.0013	0.0012	0.0012	0.0012	0.0013	0.0012
SnI_2	0.0011	0.0010	0.0010	0.0010	0.00095	0.0010	0.0010	0.0010
PbF_2	0.0031	0.0030	0.0028	0.0027	0.0028	0.0027	0.0029	0.0028
$PbCl_2$	0.0017	0.0016	0.0016	0.0016	0.0016	0.0015	0.0016	0.0015
$PbBr_2$	0.0012	0.0011	0.0011	0.0011	0.0010	0.0010	0.0011	0.0010
PbI_2	0.00091	0.00085	0.00084	0.00083	0.00078	0.00078	0.00083	0.0010

tion energies for some of the dihalides. As it can be seen in Figure 5a, the multireference (MRCI) and the hybrid BDEs have essentially the same trends, with some discrepancies when compared with the values reported by Benavides-García.[34] DFT underestimates the BDEs. On the other hand, it is noticeable that the BDEs reported by Huheey, corresponding to GeX_2 and SnX_2, are essentially the same (see Figure 5a). This contrasts with the behavior obtained with the present methodology, where the Sn−X BDE is smaller than that calculated for Ge−X. For the tetrahalides (see Figure 5b), the similarity between the values reported by Huheey and the present results is more evident. The most important difference is that the QR-DFT BDEs of CBr_4 and CI_4 are smaller than those available in the literature. Again, as for the dissociation energies, and for both di- and tetrahalides, the Si−X bond dissociation energy is the largest for a given set of halides. Thus, in general, the dissociation energies and the mean bond dissociation energies calculated within a DFT pseudopotential approach follow the experimental trends along the group. From the comparison with available experimental information, it is found that the semilocal and hybrid exchange-correlation functionals provide the best numerical values for these energy differences.

Disproportionation reactions, that are defined as

$$2MX_2(g) \rightarrow MX_4(g) + M(g), \quad \Delta U_d \tag{3}$$

have been used by several authors[35] to analyze the valence preference of some groups in the periodic table. The values obtained for this reaction energy, including ZPE and atomic-SO, are shown in Table 14 (see also Figure 6). Contrary to the expected behavior of a reaction where an isolated atom is involved, the energy differences provided by LSDA are numerically very close to those predicted by the semilocal functional.

TABLE 12: Zero-Point Energies (in Atomic Units) of MX_4 Molecules Calculated at Hartree−Fock (HF), Local (LSDA), Semilocal (BLYP), and Hybrid (B3LYP) Theoretical Levels

	HF		LSDA		BLYP		B3LYP	
molecule	NR	QR	NR	QR	NR	QR	NR	QR
CF_4	0.019	0.019	0.017	0.017	0.016	0.016	0.017	0.017
CCl_4	0.011	0.011	0.0093	0.0092	0.0086	0.0085	0.0093	0.0092
CBr_4	0.0076	0.0079	0.0065	0.0068	0.0059	0.0063	0.0064	0.0068
CI_4	0.0058	0.0061	0.0048	0.0053	0.0043	0.0048	0.0048	0.0052
SiF_4	0.013	0.014	0.012	0.012	0.012	0.012	0.012	0.013
$SiCl_4$	0.0078	0.0078	0.0072	0.0071	0.0070	0.0069	0.0073	0.0072
$SiCl_4$	0.0056	0.0056	0.0051	0.0051	0.0048	0.0049	0.0051	0.0051
SiI_4	0.0044	0.0043	0.0040	0.0040	0.0037	0.0037	0.0039	0.0039
GeF_4	0.010	0.010	0.0090	0.0091	0.0088	0.0090	0.0092	0.0094
$GeCl_4$	0.0060	0.0060	0.0054	0.0053	0.0052	0.0051	0.0054	0.0054
$GeBr_4$	0.0041	0.0041	0.0037	0.0037	0.0034	0.0035	0.0037	0.0037
GeI_4	0.0032	0.0031	0.0028	0.0028	0.0026	0.0026	0.0028	0.0028
SnF_4	0.0093	0.0088	0.0083	0.0077	0.0083	0.0076	0.0086	0.0079
$SnCl_4$	0.0054	0.0050	0.0049	0.0045	0.0047	0.0043	0.0050	0.0046
$SnBr_4$	0.0036	0.0034	0.0032	0.0031	0.0031	0.0030	0.0033	0.0031
SnI_4	0.0027	0.0026	0.0025	0.0024	0.0023	0.0022	0.0025	0.0024
PbF_4	0.0080	0.0077	0.0069	0.0064	0.0068	0.0062	0.0072	0.0067
$PbCl_4$	0.0046	0.0044	0.0041	0.0037	0.0040	0.0036	0.0042	0.0038
$PbBr_4$	0.0030	0.0029	0.0027	0.0025	0.0026	0.0024	0.0027	0.0025
PbI_4	0.0023	0.0022	0.0020	0.0019	0.0019	0.0018	0.0020	0.0019

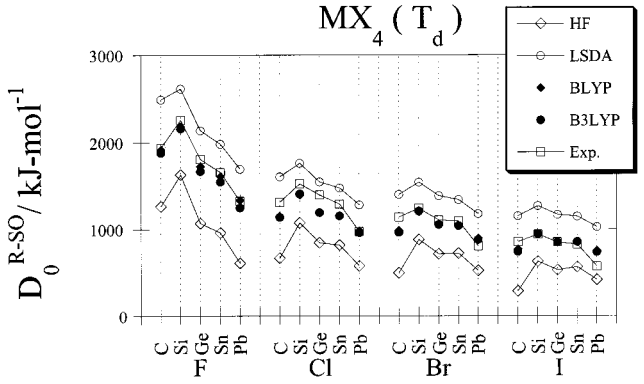

Figure 4. Dissociation energies, including zero-point energies and atomic spin−orbit corrections, of group 14 tetrahalides with tetrahedral symmetry (T_d), calculated with quasirelativistic effective core potentials and at Hartree−Fock (HF), local (LSDA), semilocal (BLYP), and hybrid (B3LYP) levels.

On going down in the periodic table, the differences between the predicted DFT disproportionation energies become smaller. Notice that, for lead, the BLYP ΔU_d is actually closer to B3LYP than to the local values. One can also see that HF disproportionation energies are severely underestimated, even becoming negative in some cases.

IV. Roles of Relativity and the Exchange-Correlation Energy Functional

The effects of scalar relativistic contributions and the nature of the exchange-correlation energy functional on the calculation of the structural and energetical parameters of group 14 halides are analyzed in this section. The relativistic correction on a given property is estimated according to the usual expression

$$\Delta_R(\text{property}) = \text{property}^{\text{relativistic}} - \text{property}^{\text{nonrelativistic}} \quad (4)$$

The effect of the scalar relativistic contributions on the molecular geometries of MX_2 and MX_4 (T_d) can be fully appreciated in Figure 7. From this figure, it can be seen that, in general, the most important bond contractions occur with the bromides and iodines. For fluorides and chlorides, relativity produces a bond dilation, being largest in the tin halides. For bromides and iodines, and excluding Sn, there is a bond contraction that increases as one descends in group 14. For the tetrahalides with T_d symmetry, and, more specifically, for bromides and iodines, bond contractions for C, Si, and Ge are considerably larger than those observed in the MX_2 molecules. The differences between the relativistic effects predicted in the bond distances with different exchange-correlation functionals vary in a very narrow range. In some cases, large differences are obtained between HF and DFT (see PbX_2 in Figure 7a and PbX_4 in Figure 7b). As can be seen in Figure 7, Sn clearly breaks the expected tendency in the bond contractions when one moves down in the group. This anomalous behavior points toward a revision of the ECP of this element or to the possible contribution of core polarization effects in tin compounds. Both aspects deserve future attention.

The effect of relativity on the bond angles of the dihalides is depicted in Figure 8. For the heavy halogens (Br and I) and for carbon to tin, the scalar relativistic contributions make the bond angles of these molecules smaller than those predicted with the nonrelativistic ECP. CI_2 has the largest contraction. At the HF level, the CI_2 bond angle decreases by almost 8°, while the DFT methods predict a bond angle contraction of about 5°. This relativistic bond angle reduction for the carbon through tin dihalides is independent of the theoretical method used to optimize the molecular structures. As expected, relativity has a practically negligible effect on the carbon to germanium difluorides and dichlorides. The behavior of lead halides is completely different. For all PbX_2 compounds and with all methods, the quasirelativistic ECP predicts an increase in the bond angle. The largest dilation is obtained for $PbCl_2$ (∼3°). For the heavier halogens (bromine and iodine), the bond angle expansion is about 2°.

The global effect of density inhomogeneities, and the asymptotic behavior of the KS effective potential on the calculation of structural and energetical molecular parameters, can be assessed by the following expression:

$$\Delta_{\text{DFT}-\text{HF}}(\text{property}) = \text{property}_{\text{DFT}}^{\text{nonrelativistic}} - \text{property}_{\text{HF}}^{\text{nonrelativistic}} \quad (5)$$

TABLE 13: Mean Bond Energies (in kJ mol) Obtained from the Dissociation Energies of MX_2 and MX_4, Calculated at Hartree−Fock (HF), Local (LSDA), Semilocal (BLYP), and Hybrid (B3LYP) Theoretical Levels, Including Zero-Point Energy and Atomic Spin−Orbit Corrections

	HF		LSDA		BLYP		B3LYP		expt	
bond	MX_2	MX_4	MX_2	MX_4	MX_2	MX_4	MX_2	MX_4	MX_2	MX_4
CF	310.63	314.16	668.49	621.73	520.78	476.89	503.53	468.25	485	485
CCl	166.93	163.06	454.00	397.69	338.24	283.89	324.63	280.48	328	328
CBr	108.09	109.24	391.68	335.61	285.48	231.18	268.92	226.25	285	285
CI	32.71	41.14	313.53	257.82	214.54	160.94	195.00	154.75	213	213
SiF	396.49	405.70	683.31	652.50	572.72	544.85	560.20	538.45	565	565
SiCl	272.92	265.05	482.80	436.51	391.54	344.95	387.93	348.33	381	381
SiBr	218.72	205.39	421.45	371.04	336.44	285.17	331.90	287.48	310	310
SiI	142.36	126.63	340.49	286.90	259.10	204.19	253.18	205.45	234	234
GeF	291.81	260.69	597.99	527.87	491.01	424.38	471.28	410.10	481	452
GeCl	234.90	202.56	447.73	378.09	358.74	289.38	353.11	289.70	385	349
GeBr	193.15	159.50	395.79	326.71	312.64	243.62	307.07	243.68	325	276
GeI	128.15	97.02	323.68	256.80	243.62	176.85	237.57	176.54	264	212
SnF	257.43	228.39	548.41	484.54	450.98	391.01	430.97	375.33	481	414
SnCl	220.19	190.93	418.89	355.42	337.92	275.65	332.63	275.04	386	323
SnBr	184.30	156.36	371.44	310.47	295.39	235.12	290.79	235.20	329	273
SnI	125.08	101.14	303.85	246.92	229.57	172.85	225.16	173.40	261	205
PbF	180.03	121.12	473.95	392.65	378.28	302.59	356.63	281.27	394	331
PbCl	167.58	111.32	364.75	287.62	286.36	212.58	280.53	207.04	304	243
PbBr	137.57	86.97	321.70	250.47	248.10	179.83	243.41	175.69	260	201
PbI	84.91	44.56	259.27	197.10	187.03	127.56	183.11	124.74	205	142

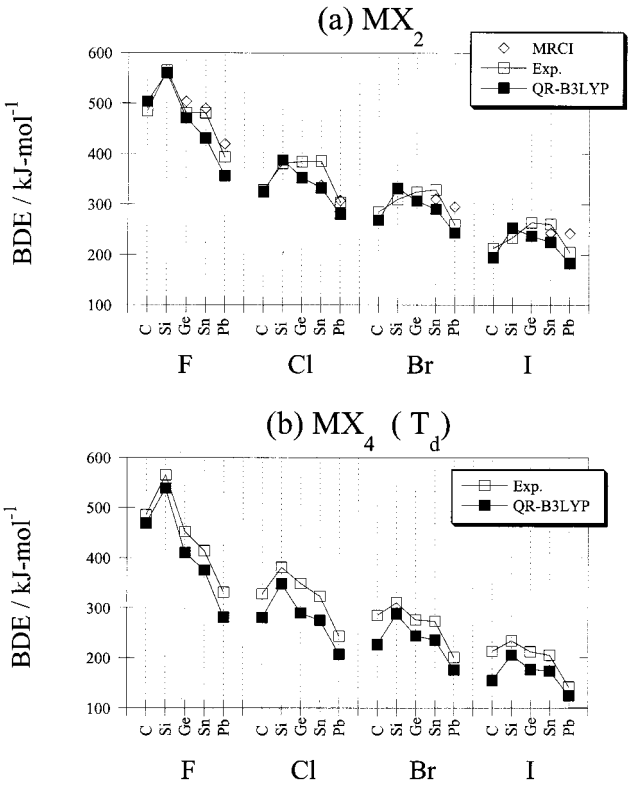

Figure 5. Bond dissociation energies (BDE) obtained from the dissociation reaction of the corresponding group 14 for (a) dihalides and (b) tetrahalides, and calculated with quasirelativistic effective core potentials and using the hybrid (B3LYP) exchange-correlation energy functional. All values include the zero-point energies and the atomic spin−orbit corrections.

This analysis simply aims to extract the trends that are obtained when one uses different exchange-correlation energy functionals in calculating the structural and energetic molecular parameters of group 14 halides. It is worth noting that, when property = total energy, eq 5 has been used[26] to measure the pure nonrelativistic correlation energy contribution using Moller−Plesset and coupled cluster as well as hybrid functionals.

TABLE 14: Disproportionation Reaction Energies (in kJ mol) Calculated at Hartree−Fock (HF), Local (LSDA), Semilocal (BLYP), and Hybrid (B3LYP) Theoretical Levels, Including Zero-Point Energy and Atomic Spin−Orbit Corrections

molecule	HF	LSDA	BLYP	B3LYP
CF_2	−14.1	186.9	175.5	141.0
CCl_2	15.4	225.1	217.3	176.5
CBr_2	−4.6	224.2	217.1	170.6
CI_2	−33.7	222.7	214.3	160.9
SiF_2	−36.8	123.2	111.4	87.0
$SiCl_2$	31.5	185.0	186.2	158.3
$SiBr_2$	53.3	201.5	205.0	177.6
SiI_2	62.9	214.3	219.5	190.8
GeF_2	163.0	318.9	305.0	283.2
$GeCl_2$	167.8	317.0	315.9	292.1
$GeBr_2$	173.1	314.8	314.5	292.0
GeI_2	163.0	305.9	305.5	282.6
SnF_2	193.3	332.5	316.9	299.6
$SnCl_2$	194.1	330.9	326.1	307.3
$SnBr_2$	188.9	320.9	318.1	299.4
SnI_2	172.8	304.7	303.9	284.1
PbF_2	466.9	556.4	534.0	532.7
$PbCl_2$	456.3	539.8	526.4	525.2
$PbBr_2$	433.8	516.2	504.3	502.1
PbI_2	392.8	480.0	469.2	464.8

However, eq 5 is not a proper definition that allows one to thoroughly understand the effect of correlation in Kohn−Sham theory.[36] Δ_{DFT-HF} for the bond distances of MX_2 and MX_4 is depicted in Figure 9. The first aspect to be noted from this figure is that all nonrelativistic DFT methods predict larger bond distances than HF. As can also be appreciated, the semilocal exchange-correlation functional exhibits the largest deviation from HF. Interestingly, the LSDA Δ_{DFT-HF}(bond distance) decreases as the halogen atom becomes heavier, contrasting with an opposite behavior provided by the semilocal functional. There is only one exception to this behavior, namely, the trend obtained for CX_2 with LSDA. The behavior of the hybrid functional is smoother than that observed with the other two functionals, showing a narrower variation when changing the halogen atom. Thus, one can conclude that (a) for a given element belonging

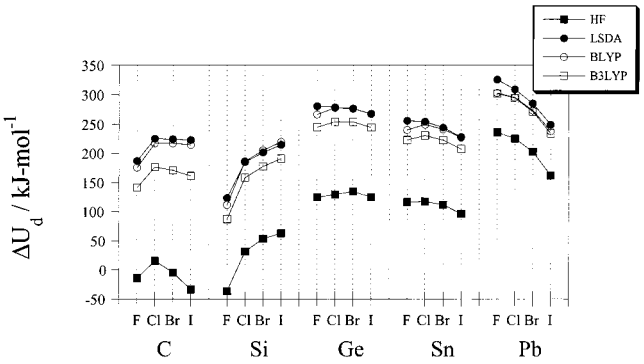

Figure 6. Disproportionation reaction energies (see reaction 3), including zero-point energies and atomic spin−orbit corrections, of group 14 halides, calculated with quasirelativistic effective core potentials and at Hartree−Fock (HF), local (LSDA), semilocal (BLYP), and hybrid (B3LYP) levels.

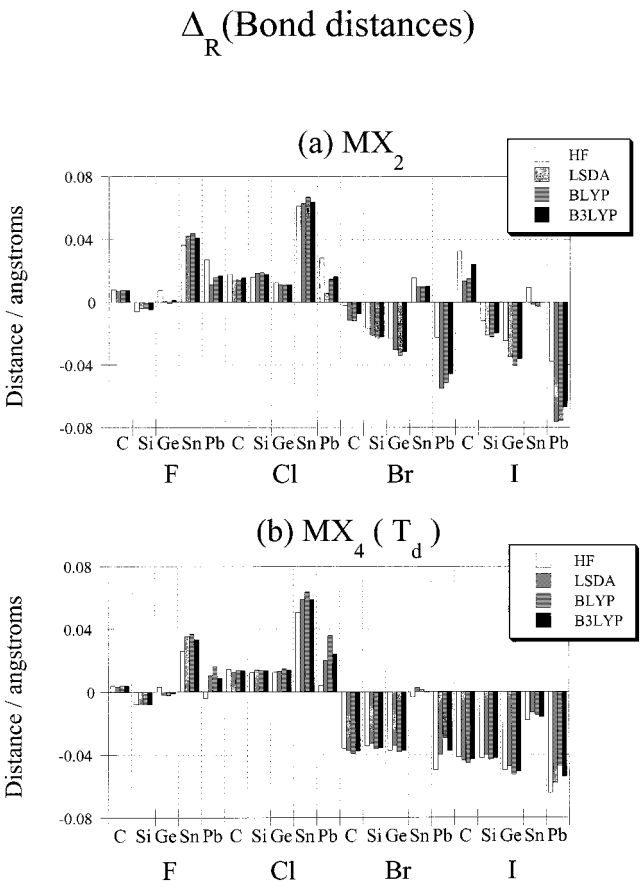

Figure 7. Relativistic effects (see eq 4) in the bond distances of group 14 (a) dihalides and (b) tetrahalides with tetrahedral (T_d) symmetry and using the following theoretical levels: Hartree−Fock (HF), local (LSDA), semilocal (BLYP), and hybrid (B3LYP).

to group 14, the bond distances predicted with LSDA are closer to HF when the halogen atom is heavier, (b) density inhomogeneities incorporated through the semilocal approximation provide the opposite trend to that described in (a), and finally, (c) the presence of HF-like exchange smoothens the behavior of Δ_{DFT-HF}(bond distance). Overall, the nature of the functional predicts different behaviors.

Δ_{DFT-HF} for the bond angles of MX_2 is depicted in Figure 10. Carbon has a very different behavior than the rest of the elements in group 14. For this element, all functionals tested have the same trend, namely, to decrease the halogen−carbon−halogen angle compared to the HF value, ongoing from fluorine

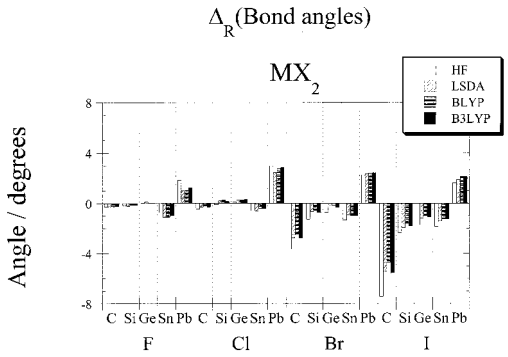

Figure 8. Relativistic effects (see eq 4) in the bond angles of group 14 dihalides, using the following theoretical levels: Hartree−Fock (HF), local (LSDA), semilocal (BLYP), and hybrid (B3LYP).

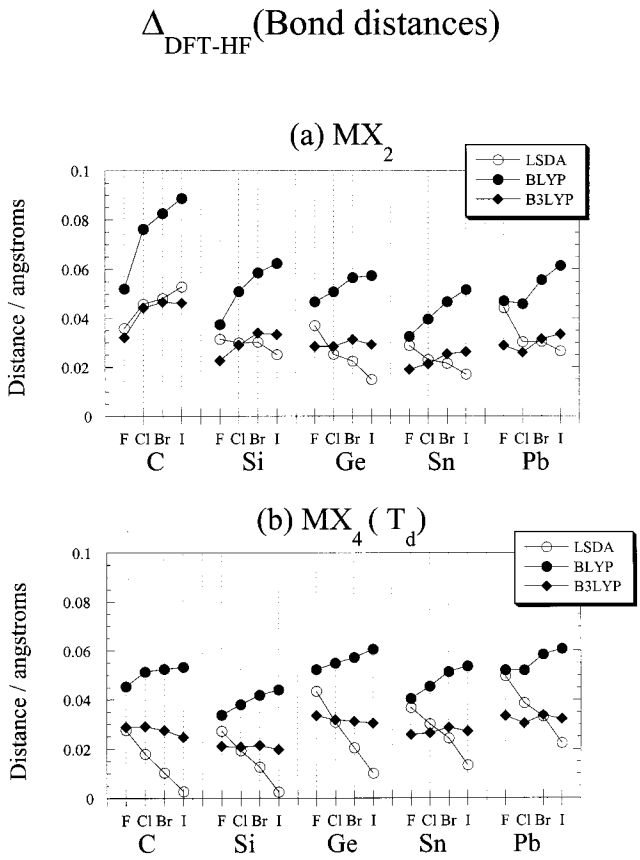

Figure 9. Difference between DFT and HF (see eq 5) bond distances of group 14 (a) dihalides and (b) tetrahalides with tetrahedral (T_d) symmetry and using the following exchange-correlation energy functionals: local (LSDA), semilocal (BLYP), and hybrid (B3LYP).

to iodine. For silicon through tin, one can see that the semilocal functional has the largest deviations from HF and has a minimum for MBr_2 that is present in all exchange-correlation functionals tested in this work.

Turning to energetics, special emphasis will be given to the influence of scalar relativistic effects, spin−orbit, and exchange-correlation energy functionals in the calculation of the energy differences presented in the previous section. If the atomic spin−orbit contribution is not included, the behavior of the relativistic correction to the dissociation energy does not follow the expected trend. This is illustrated in Figure 11a for MBr_2. After incorporating the atomic spin−orbit correction, one obtains the expected behavior depicted in Figure 11b, again taking the dibromides as an illustrative example.

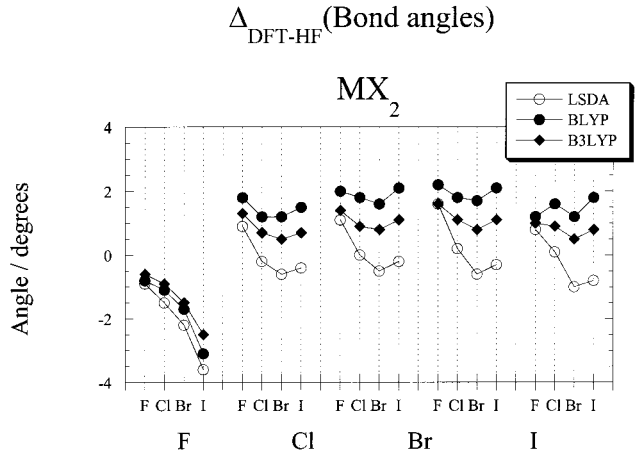

Figure 10. Difference between DFT and HF (see eq 5) bond angles of group 14 dihalides, using the following exchange-correlation energy functionals: local (LSDA), semilocal (BLYP), and hybrid (B3LYP).

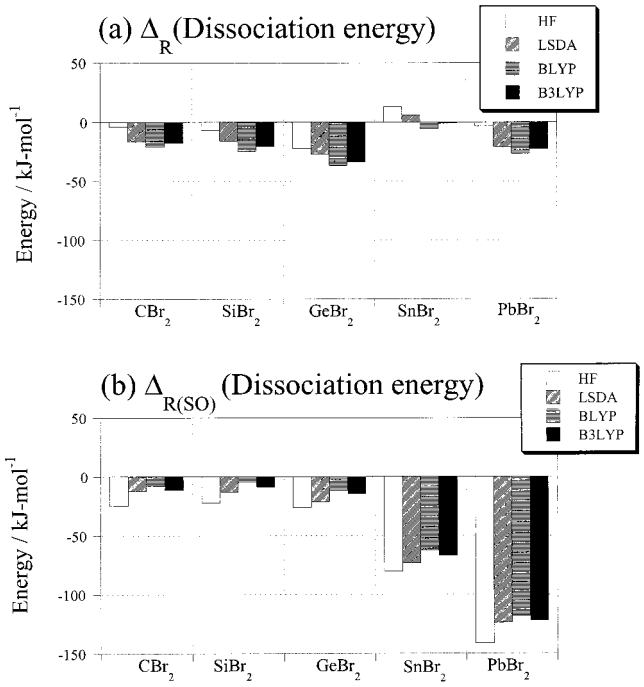

Figure 11. Relativistic effects (see eq 4) in the dissociation energies of group 14 dibromides, using Hartree−Fock (HF), local (LSDA), semilocal (BLYP), and hybrid (B3LYP), (a) without and (b) including the atomic spin−orbit correction.

The role of the exchange-correlation energy functional used in the calculation of dissociation energies can be analyzed in Figure 12, where the MX_4 $\Delta_{DFT-HF}(D_0)$ is depicted. In all cases, the chemical bonds between group 14 elements and halogens predicted by DFT are stronger than HF. Interestingly, the fluorides are the most affected, and even though there is a decreasing tendency when one moves down to iodine, the effect in the chlorides, bromides, and iodines is essentially the same. This pronounced effect in fluorine-containing molecules provides additional evidence of the importance of correlation in this atom. Several works have pointed out the anomalous behavior of fluorine in the DFT calculation of several properties.[37] The largest difference with respect to HF corresponds to LSDA. The semilocal and hybrid functionals have practically the same differences with respect to HF. The trends are very similar to those obtained at the local level. The dihalides show a very similar behavior.

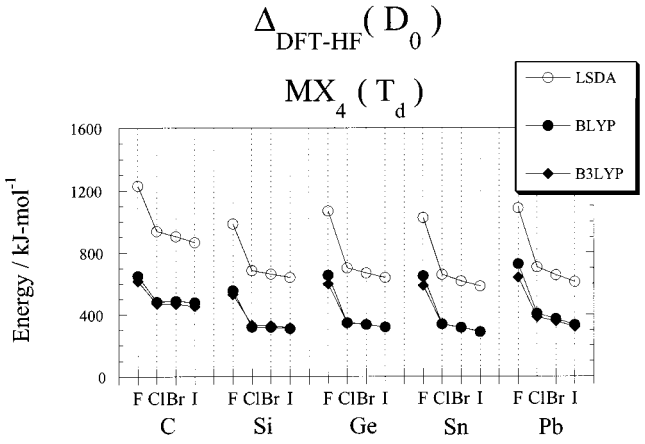

Figure 12. Difference between DFT and HF (see eq 5) zero-point energy corrected dissociation energies of group 14 tetrahalides with tetrahedral (T_d) symmetry, using the following exchange-correlation energy functionals: local (LSDA), semilocal (BLYP), and hybrid (B3LYP).

V. Conclusions

An exhaustive density functional and pseudopotential study of the structure and energetics of group 14 halides is presented, focusing on the ability of different quantum chemical models in describing these properties. After comparison with experiment and high-level ab initio calculations, it is found that the Hartree−Fock and the local spin density approximation to the exchange-correlation energy functional provide the best geometrical parameters of group 14 dihalides and tetrahalides, in the singlet electronic state. The hybrid functional (B3LYP) is very close behind. In view of the good geometrical description obtained for these molecules, it is concluded that the experimental bond distance and bond angle of CBr_2 has to be revised. All density functional dissociation energies follow the experimental trends and show the well-known behavior: the local spin density approximation overestimates the binding, which is reduced by the semilocal and hybrid approaches. The inclusion of atomic spin−orbit correction does not change the trends, but it is fundamental to produce dissociation energies in better agreement with experiment. The analysis of the energy differences associated with the disproportionation reactions establishes that, contrary to the expected behavior of a reaction where an isolated atom is involved, the values provided by the local functional are numerically very close to those predicted with the semilocal exchange correlation energy functional.

Acknowledgment. We thank Dra. Laura Gasque for motivating this work. Computer time granted at the Laboratorio de Visualización y Cómputo Paralelo, UAM-Iztapalapa, is gratefully acknowledged. S.E. and R.V. acknowledge financial support provided by a CONACYT fellowship.

References and Notes

(1) Tyagi, M. S. *Introduction to Semiconductor Materials and Devices*; John Wiley and Sons: New York, 1991.

(2) Sherman, A. *Chemical Vapor Deposition for Microelectronics. Principles, Technology, and Applications*; Noyes Publications: Park Ridge, New Jersey, 1987.

(3) Kirmse, W. *Carbene Chemistry*; Academic Press: New York, 1971.

(4) Greenwood, N. N.; Earnshaw, A. *Chemistry of the Elements*; Pergamon Press: Oxford, 1984.

(5) Tachibana, A.; Kurosaki, Y.; Kawauchi, S.; Yamabe, T. *J. Phys. Chem.* **1991**, *95*, 1716.

(6) Tachibana, A.; Kawauchi, S.; Yamabe, T. *J. Phys. Chem.* **1991**, *95*, 2471−2476.

(7) Dyall, K. G.; Faegri, K. J.; Taylor, P. R.; Partridge, H. *J. Chem. Phys.* **1991**, *95*, 2583.
(8) Dyall, K. G. *J. Chem. Phys.* **1992**, *96*, 1210.
(9) Dyall, K. G. *J. Chem. Phys.* **1993**, *98*, 2191.
(10) Almlöf, J.; Gropen, O. Relativistic Effects in Chemistry. In *Reviews in Computational Chemistry*; Lipkowitz, K. B., Boyd, D. B., Eds.; VCH Publishers: New York, 1996; Vol. 8, pp 203−244.
(11) Kohn, W.; Becke, A. D.; Parr, R. G. *J. Phys. Chem.* **1996**, *100*, 12974.
(12) Gill, P. M.; Johnson, B. G.; Pople, J. A.; Frisch, M. *Chem. Phys. Lett.* **1992**, *197*, 499.
(13) Handy, N. C.; Maslen, P. E.; Amos, R. D.; Andrews, J. S.; Murray, C. W.; Laming, G. *Chem. Phys. Lett.* **1992**, *197*, 506.
(14) Johnson, B. G.; Gill, P. M. W.; Pople, J. A. *Chem. Phys. Lett.* **1993**, *98*, 5612.
(15) Frenking, G.; Antes, I.; Boehme, M.; Dapprich, S.; Ehlers, A. W.; Jonas, V.; Neuhaus, A.; Otto, M.; Stegmann, R.; Veldkamp, A.; Vyboishchikov, S. F. Pseudopotential calculations of transition metal compounds: scope and limitations. In *Reviews in Computational Chemistry*; Lipkowitz, K. B., Boyd, D. B., Eds.; VCH Publishers: New York, 1996; Vol. 8, pp 63−143.
(16) Cundari, T. R.; Benson, M. T.; Leigh Lutz, M.; Sommerer, S. O. Effective core potential approaches to the chemistry of the heavier elements. In *Reviews in Computational Chemistry*; Lipkowitz, K. B., Boyd, D. B., Eds.; VCH Publishers: New York, 1996; Vol. 8, pp 145−202.
(17) Vosko, S. H.; Wilk, L.; Nusair, M. *Can. J. Phys.* **1980**, *58*, 1200.
(18) Becke, A. D. *Phys. Rev. A* **1988**, *38*, 3098.
(19) Lee, C.; Yang, W.; Parr, R. G. *Phys. Rev. B* **1988**, *37*, 785.
(20) Becke, A. D. *J. Chem. Phys.* **1993**, *98*, 5648.
(21) Bergner, A.; Dolg, M.; Küchle, W.; Stoll, H.; Preuss, H. *Mol. Phys.* **1993**, *80*, 1431.
(22) The polarization functions were obtained from the Extensible Computational Chemistry Environment Basis Set Database, version 1.0, as developed and distributed by the Molecular Science Facility, Environmental and Molecular Sciences Laboratory, which is part of the Pacific Northwest Laboratory, P.O. Box 999, Richland, WA 99352, and funded by the U.S. Department of Energy. The Pacific Northwest Laboratory is a multiprogram laboratory operated by Battelle Memorial Institue for the U.S. Department of Energy under Contract DE-AC06−76RLO 1830. Contact David Feller, Karen Schuchardt, or Don Jones for further information. This information can be reached at http://www.emsl.pnl.gov:2080/docs/homepage.html.
(23) Schafer, A.; Horn, H.; Ahlrichs, R. *J. Chem. Phys.* **1992**, *97*, 2571.
(24) Huzinaga, S.; Andzelm, J.; Klobukowski, M.; Radzio-Andzelm, E.; Sakai, Y.; Tatewaki, H. *Gaussian Basis Sets for Molecular Calculations*; Elsevier: Amsterdam, 1984.
(25) Russo, T. V.; Martin, R. L.; Hay, P. J. *J. Phys. Chem.* **1995**, *99*, 17085.
(26) Hrusak, J.; Hertwig, R. H.; Schroder, D.; Schwerdtfeger, P.; Koch, W.; Schwarz, H. *Organometallics* **1995**, *14*, 1284.
(27) Wang, S. G.; Schwarz, W. H. E. *J. Mol. Struct. (THEOCHEM)* **1995**, *338*, 347.
(28) Frisch, M. J.; Trucks, G. W. S.; H. B.; Gill, P. M. W.; Johnson, B. G.; Robb, M. A.; Cheeseman, J. R.; Keith, T.; Petersson, G. A.; Montgomery, J. A.; Raghavachari, K.; Al-Laham, M. A.; Zakrzewski, V. G.; Ortiz, J. V.; Foresman, J. B.; Cioslowsky, J.; Ayala, P. Y.; Chen, W.; Wong, M. W. *Gaussian 94*, revision D.3; Gaussian, Inc.: Pittsburgh, PA, 1995.
(29) Dolg, M. *Mol. Phys.* **1996**, *88*, 1645.
(30) Hargittai, M. *Coord. Chem. Rev.* **1988**, *91*, 35.
(31) Quantum Chemistry Literature Data Base; http://qcldb.ims.ac.jp.
(32) Moore, C. E. Atomic Energy Levels. Natl. Bur. Stand. (U.S.), Circ. No 467; U.S. GPO: Washington, D.C., 1958.
(33) Huheey, J. E.; Keiter, E. A.; Keiter, R. L. *Inorganic Chemistry*, 4th ed.; Harper Collins: New York, 1990.
(34) Benavides-García, M.; Balasubramanian, K. *J. Chem. Phys.* **1992**, *97*, 7537.
(35) Schwerdtfeger, P.; Heath, G. A.; Dolg, M.; Bennett, M. A. *J. Am. Chem. Soc.* **1992**, *114*, 7518.
(36) Baerends, E. J.; Gritsenko, O. V. *J. Phys. Chem.* **1997**, *101*, 5383.
(37) Proynov, E. I.; Ruiz, E.; Vela, A.; Salahub, D. R. *Int. J. Quantum Chem.* **1995**, *S29*, 61.
(38) Huber, K. P.; Herzberg, G. *Molecular Spectra and Molecular Structure Constants of Diatomic Molecules*; Van Nostrand: New York, 1979.
(39) Peterson, K. A.; Mayrhofer, R. C.; Sibert, E. L., III; Woods, R. C. *J. Chem. Phys.* **1991**, *94*, 414.
(40) Bauschlicher, C. W., Jr.; Schaefer, H. F., III; Bagus, P. S. *J. Am. Chem. Soc.* **1977**, *99*, 7106.
(41) Cameron, M. R.; Kable, S. H.; Bacskay, G. B. *J. Chem. Phys.* **1995**, *103*, 4476.
(42) Kim, S.-J.; Hamilton, T. P.; Scheffer, H. F., III *J. Chem. Phys.* **1991**, *94*, 2063.
(43) Bauschlicher, C. W., Jr. *J. Am. Chem. Soc.* **1980**, *102*, 5492.
(44) Colvin, M. E.; Grev, R. S.; Schaefer, H. F., III *Chem. Phys. Lett.* **1983**, *99*, 399.
(45) Johnson, R. D., III; Hudgens, J. W.; Ashfold, M. N. R. *Chem. Phys. Lett.* **1996**, *261*, 474.
(46) Shin, S. K.; Goddard, W. A., III; Beauchamp, J. L. *J. Phys. Chem.* **1990**, *94*, 6963.
(47) Bock, H.; Kremer, M.; Dolg, M.; Preuss, H.-W. *Angew. Chem., Int. Ed. Engl.* **1991**, *30*, 1186.
(48) Spoliti, M.; Ramondo, F.; Bencivenni, L.; Kolandaivel, P.; Kumaresan, R. *J. Mol. Struct. (THEOCHEM)* **1993**, *283*, 73.
(49) Karolczak, J.; Grev, R. S.; Clouthier, D. J. *J. Chem. Phys.* **1994**, *101*, 891.
(50) Dai, D.; Al-Zahrani, M.; Balasubramanian, K. *J. Phys. Chem.* **1994**, *98*, 9233.
(51) Tsuchiya, M. J.; Honjou, H.; Tanaka, K.; Tanaka, T. *J. Mol. Struct.* **1995**, *352/352*, 407.
(52) Chen, H.; Krasowski, M.; Fitzgerald, G. *J. Chem. Phys.* **1993**, *98*, 8710.
(53) Giricheva, N. I.; Girichev, G. V.; Shlykov, S. A.; Titov, V. A.; Chusova, T. P. *J. Mol. Struct.* **1995**, *344*, 127.
(54) Fjeldberg, T.; Haaland, A.; Schilling, B. E. R.; Lappert, M. F.; Thorne, A. J. *J. Chem. Soc., Dalton Trans.* **1986**, 1551.
(55) Trinquier, G.; Barthelat, J.-C. *J. Am. Chem. Soc.* **1990**, *112*, 9121.
(56) Benavides-García, M.; Balasubramanian, K. *J. Chem. Phys.* **1994**, *100*, 2821.
(57) Gutsev, G. L.; Ziegler, T. *J. Phys. Chem.* **1991**, *95*, 7220.
(58) Dixon, D. A.; Arduengo, A. J., III *J. Phys. Chem.* **1987**, *91*, 3195.
(59) Jonas, V.; Frenking, G.; Reetz, M. T. *J. Comput. Chem.* **1992**, *13*, 935.
(60) Roszak, S.; Vijayakumar, M.; Balasubramanian, K.; Koski, W. S. *Chem. Phys. Lett.* **1993**, *208*, 225.
(61) Roszak, S.; Kaufman, J. J.; Koski, W. S.; Vijayakumar, M.; Balasubramanian, K. *J. Chem. Phys.* **1994**, *101*, 2978.
(62) Su, M.-D.; Schlegel, H. B. *J. Phys. Chem.* **1993**, *97*, 8732.
(63) Schulz, A.; Klapotke, T. M. *Spectrochim. Acta* **1995**, *51A*, 905.
(64) Puhakka, E.; Hirva, P.; Pakkanen, T. A. *J. Mol. Struct. (THEOCHEM)* **1995**, *333*, 79.
(65) Hyde, R. G.; Peel, J. B. *Mol. Phys.* **1977**, *33*, 887.
(66) Shimoni-Livny, L.; Glusker, J. P.; Bock, C. W. *Inorg. Chem.* **1998**, *37*, 1853.
(67) Ehrhardt, B. K.; Ystenes, M. *Spectrochim. Acta* **1995**, *51A*, 699.